

QASIM, M., AYOUB, M., SINGH, K., INAYAT, A., SHAMSUDDIN, R., DANISH, M. and FARRUKH, S. 2023. A comparative study of eggshell and commercial sorbent-based catalysts through synthesis and characterization for SESR process. *Sustainability* [online], 15(20), article number 14762. Available from: <https://doi.org/10.3390/su152014762>






A comparative study of eggshell and commercial sorbent-based catalysts through synthesis and characterization for SESR process.

QASIM, M., AYOUB, M., SINGH, K., INAYAT, A., SHAMSUDDIN, R.,
DANISH, M. and FARRUKH, S.

2023

Article

A Comparative Study of Eggshell and Commercial Sorbent-Based Catalysts through Synthesis and Characterization for SESR Process

Muhammad Qasim ^{1,2}, Muhammad Ayoub ^{1,2,*} , Karamjit Singh ², Abrar Inayat ³ , Rashid Shamsuddin ^{1,2} , Mohammed Danish ⁴  and Sarah Farrukh ⁵ 

- ¹ HiCoE, Centre for Biofuel and Biochemical Research (CBBR), Institute of Self-Sustainable Building (ISB), Universiti Teknologi PETRONAS (UTP), Seri Iskandar 32610, Perak, Malaysia; qasimazam4@gmail.com (M.Q.); mrashids@utp.edu.my (R.S.)
- ² Department of Chemical Engineering, Universiti Teknologi PETRONAS, Bandar Seri Iskandar 32610, Perak, Malaysia; karamjit_17001821@utp.edu.my
- ³ Department of Sustainable & Renewable Energy Engineering, University of Sharjah, Sharjah 27272, United Arab Emirates; ainayat@sharjah.ac.ae
- ⁴ School of Industrial Technology, Universiti Sains Malaysia, Minden Campus, Penang 11800, Pulau Pinang, Malaysia; danish@usm.my
- ⁵ Department of Chemical Engineering, School of Chemical and Materials Engineering, National University of Sciences and Technology, Islamabad 44000, Pakistan; sarah.farrukh@scme.nust.edu.pk or sfarrukh@ed.ac.uk
- * Correspondence: muhammad.ayoub@utp.edu.my



Citation: Qasim, M.; Ayoub, M.; Singh, K.; Inayat, A.; Shamsuddin, R.; Danish, M.; Farrukh, S. A Comparative Study of Eggshell and Commercial Sorbent-Based Catalysts through Synthesis and Characterization for SESR Process. *Sustainability* **2023**, *15*, 14762. <https://doi.org/10.3390/su152014762>

Academic Editors: Pei Sean Goh, Ahmad Fauzi Ismail, Jun-Wei Lim, Hooi Siang Kang and Jose Navarro Pedreño

Received: 13 June 2023

Revised: 21 August 2023

Accepted: 30 August 2023

Published: 11 October 2023



Copyright: © 2023 by the authors. Licensee MDPI, Basel, Switzerland. This article is an open access article distributed under the terms and conditions of the Creative Commons Attribution (CC BY) license (<https://creativecommons.org/licenses/by/4.0/>).

Abstract: Hydrogen is a clean and valuable energy carrier, and there is growing consensus that a hydrogen-based economy could be the key to ensuring the long-term reliability and environmental friendliness of the world's energy supply. There are a variety of methods and technologies that may be used to produce hydrogen; among them, sorption-enhanced steam reforming is regarded as the way that is the most effective. For the purpose of making a decision about which catalysts to employ in SESR in the future, this study compared three distinct kinds of catalysts. The wet impregnation method was used to manufacture the waste-derived CaO-implemented Ni-based catalysts, which were then used in sorption-enhanced steam reforming (SESR) to produce hydrogen (H₂). X-ray diffractometry (XRD), field emission scanning electron microscopy (FESEM), and thermogravimetric analyses (TGA) were used to analyze the catalysts. XRD results showed that the crystallinity behavior for all types of catalysts such as 10NMA, 10NCMA-E, and 10NCMA was identical. The spinel compounds such as NiAl₂O₄ and MgAl₂O₄ were identified in all three types of catalysts. At high temperatures, such as at 800 °C, all catalysts were stable, evident from TGA results. During three sorption cycles, the 10NCMA-based catalyst demonstrated the highest sorption capacity among the three varieties of catalysts, followed by the 10NCMA-E catalyst. During the first, second, and third calcination cycles, the 10NCMA-based catalyst released 23.88%, 22.05%, and 23.33% CO₂, respectively. 10NCMA-E can be a potential catalyst for the SESR process by decreasing the material manufacturing cost and overall cost of the SESR process.

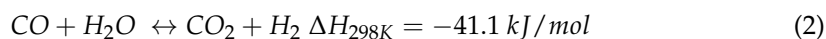
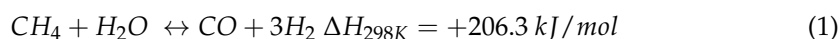
Keywords: Ni-based catalysts; waste-derived sorbent; sorption capacity; wet impregnation method

1. Introduction

Ecological issues associated with fossil fuels in energy generation drive research into hydrogen (H₂) production via sustainable and cost-effective methods [1]. For the manufacturing of urea and methyl alcohol, fuel cell technologies, and the treatment of fossil resources in numerous petroleum and chemical sectors, an enormous amount of H₂ is required [2]. In addition, H₂ has a greater heating value (140 MJ/kg) in comparison to other popular fuels; hence, it is a perfect energy carrier. Consequently, there has been a consistent

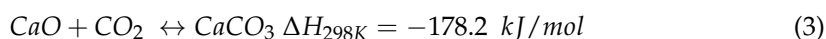
rise in the requirement for H₂ [3]. In contrast to gasoline, which has a volumetric density of 4.4 kg/m³ at standard circumstances of pressure and temperature, this substance has a volumetric density of only 0.09 kg/m³. Because of this, the fuel tank that is used to store H₂ gas must either be significantly larger or pressurized to a pressure of up to 700 bars, despite the fact that H₂ is a more reliable source of energy than other fuels such as petroleum [4,5]. In 2020, the world generated nearly 70 Mt of H₂, with 76% of that amount coming from CH₄, 23% coming from coal, and the other 1% coming from oil and power generation. This resulted in a decrease in the amount of CO₂ that was emitted into the atmosphere [6].

Coal gasification [7], thermochemical water splitting [8], chemical looping technology [9,10], direct methane decomposition [11], steam methane reforming (SMR) [12], and partial oxidation of methane [13] are established techniques for H₂ generation. Among these techniques, and despite its disadvantages, such as increased energy usage and reaction complications, SMR has been implemented at the industrial scale [14]. The SMR method consists of two reactions: reforming of methane (1) and water gas shift (2), which are endothermic and exothermic, respectively [15]. However, overall, the SMR method is an endothermic process.



Generally, the equilibrium SMR reaction produces a resultant gas with a H₂ concentration of about 70% [16]. Additionally, the process produces at least 3 kg CO₂ for each kg of CH₄ utilized [17]. In recent years, sorption-enhanced steam methane reforming (SESMR) has gained interest as a greener approach [18]. Based on Le Chatelier's principle, the combination of CO₂ capture and traditional SMR using a sorbent drives the equilibrium rate of reactions toward H₂ creation and lowers CO₂ in the output stage [19].

In previous research works, different types of SMR catalysts have been emphasized, such as those synthesized from Ni [20], Co [21], and noble metals like Ru [22], Pt [16], and Rh [23]. From an economic standpoint, noble metals are not favored [15]. Furthermore, as the reaction progresses, the activity of Ni-based catalysts reduces due to carbon deposition [24–26]. The addition of a suitable support, such as Al or Mg, increases the surface area of the catalyst and retarded carbon deposition [27,28]. Several sorbents at high temperature have been previously investigated, such as CaO [29], Li₂O₃Zr [30], Li₄O₄Si₄ [31], MgO [32], and Na₂O₃Zr [33]. Among these, sorbents based on calcium oxide (CaO) are particularly promising for a number of reasons: (i) carbonation (3) takes place at atmospheric pressure and 600–700 °C, circumstances lower than traditional SMR; and (ii) appropriate CO₂ sorption capacity and significant reactivity to CO₂ at temperatures greater than 500 °C [34]. In addition, it might be synthesized from less-expensive sources such as waste eggshell materials and possesses regeneration capabilities in SESR [35].



When the sorbent becomes depleted, a reverse carbonation process (3) regenerates the composite [36]. Production of an appropriate CO₂ sorbent is essential for the effective operation of SESMR. Moreover, the sintering process can be enhanced by integrating support into the hollow solid structure [18]. The suitability of a combined sorbent catalyst material has been demonstrated to be more effective than distinct beds of catalysts and sorbents. The idea of a combined sorbent–catalyst material has been utilized to help the exothermic and endothermic processes of SESMR balance each other out in terms of energy [37].

In the literature, it has been shown that CaO derived from waste, such as eggshells, scallop shells, and cockle shells, can be just as effective as commercial CaO-based hybrid materials [38], and that they can even outperform them in some cases [39,40]. Eggshells containing approximately 94% CaCO₃ [41] are a source of inexpensive sorbent [42]. Ac-

According to the global poultry trends, egg consumption has increased by approximately 18% over the past decade, while egg production has increased by nearly the same amount. In 2018, global production of eggs was 78 million metric tons, resulting in 8.58 million metric tons of eggshells being discarded [43]. It has been estimated that the cost of disposing of discarded eggshells generated during the processing of food is more than one million US dollars annually [44]. This expense can be avoided by employing the eggshells as a source of sorbent. Consequently, more than 40,000 tons of CaCO_3 can be obtained from 45,000 tons of eggshells yearly through food processing [45].

The literature demonstrates that eggshell-derived CaO has a greater CO_2 capture ability than commercial CaO used as a sorbent [46]. This is due to the smaller particulate size and greater subjected surface area for the adsorption reaction. It appears to be a less expensive and greener source for increased H_2 purity. In order to consider the SESR application, the CaO sorbent must be derived from eggshell waste [35] and its activity in Ni, Mg, and Al in a heating reactor must be investigated. According to the literature, a comparison between unpromoted CaO, commercial CaO, and waste-derived CaO-promoted Ni-based aluminum supported in the presence of a Mg catalyst for the application of SESR remains unexplored.

In the presence of a CaO sorbent, the opposition to carbon formation can be enhanced through a rise in single-atom carbon gasification [15]. Different types of catalysts have been investigated for the sorption-enhanced steam reforming process. However, a comparison between chicken-and-duck-eggshell-derived sorbents and commercial sorbents, promoted by and without sorbent Ni-based catalysts, has not been studied. The present study focused on synthesizing and characterizing 10NMA, 10NCMA-E, and 10NCMA catalysts for the sorption-enhanced steam reforming of glycerol. The catalysts were synthesized using a wet impregnation method and characterized via a field emission scanning electron microscope (FESEM), temperature-programmed reduction (TPR), X-ray diffraction (XRD), and thermogravimetric analysis (TGA). The comparison was carried out using all three types of catalysts over the course of three sorption cycles using a fixed-bed tubular reactor.

2. Materials and Methods

2.1. Materials and Reagents

The nitrate precursors of nickel (Ni), magnesium (Mg), and calcium (Ca) were employed in the development of catalysts. Additionally, for each type of catalyst, gamma alumina ($\gamma\text{-Al}_2\text{O}_3$) was utilized as a support material. Table 1 contains an in-depth description of each component that was consumed in the production of the catalysts.

Table 1. The description and particulars of the substances that were utilized in the synthesis of catalysts.

Material Name	Purity	CAS No	Company
Gamma alumina $\gamma\text{-Al}_2\text{O}_3$	98%	1344-28-1	Merck
Nickel (II) nitrate hexahydrate ($\text{Ni}(\text{NO}_3)_2 \cdot 6\text{H}_2\text{O}$)	98%	10031-43-3	Merck
Calcium (II) nitrate tetrahydrate ($\text{Ca}(\text{NO}_3)_2 \cdot 4\text{H}_2\text{O}$)	$\geq 99\%$	13477-34-4	Merck
Magnesium (II) nitrate hexahydrate ($\text{Mg}(\text{NO}_3)_2 \cdot 6\text{H}_2\text{O}$)	99.9%	10026-22-9	Sigma-Aldrich

2.2. Synthesis of CaO from Chicken and Duck Eggshells

The waste eggshells from chicken and duck were collected from the restaurants where they were used. After the eggshells had been broken up into smaller pieces, they were placed in a bowl of boiling water for 2 h. Following the soaking process, the membrane was taken out and given a DI water rinse. After drying in the oven at $100\text{ }^\circ\text{C}$ for 24 h, the eggshells were pulverized in a mortar to obtain very fine particles. In the final step, the powdered eggshells were calcined in an oven at $900\text{ }^\circ\text{C}$ for three and a half hours to turn the calcium carbonate into calcium oxide [47].

2.3. Characteristics of Eggshells

Eggshell is mostly made up of organic matter and the inorganic compounds carbonates, sulphates, and phosphates of calcium and magnesium. Eggshell contains amounts of Na, K, Mn, Fe, Cu, and Sr metals [48]. Eggshells have a density of approximately 2.53 g/cm³. Eggshells are primarily composed of calcium carbonate (94%), organic matter (4%), calcium phosphate (1%), and magnesium carbonate (1%) [49–51].

2.4. Preparation of Catalysts

Three types of catalysts, such as 10 wt% Ni/10 wt% Mg/ γ -Al₂O₃ (10NMA), 10 wt% Ni/5 wt% Ca/10 wt% Mg/ γ -Al₂O₃ (10NCMA-E), and 10 wt% Ni/5 wt% Ca/10 wt% Mg/ γ -Al₂O₃ (10NCMA), were synthesized using the wet impregnation method. In order to prepare the Mg-nitrate precursor solution, 10 wt% of Mg-nitrate was dissolved in DI water and added to 10 g of 10NMA catalyst. This precursor solution containing magnesium nitrate was added drop by drop to the γ -Al₂O₃ while it was continuously mixed for 3 h at room temperature. Like the Mg/ γ -Al₂O₃ solution, the Ni-precursor solution (10 wt%) was added drop by drop. After drying the resulting combination in an oven at 100 °C, a solid sample was obtained, which was then ground into powder using a porcelain mortar. The material was calcined using a ceramic crucible in a muffle furnace. The same procedure was repeated for each 10 g of the 10NCMA and 10NCMA-E catalysts. Before adding Ni-nitrate, 5 wt% Ca was added to the mixture. The difference between the 10NCMA and 10NCMA-E catalysts is only the source of calcium oxide. For the synthesis of the 10NCMA catalyst, commercially available calcium was utilized, while for 10NCMA-E the calcium was obtained from chicken and duck eggshells. All the samples were calcined at 800 °C for 6 h using a muffle furnace.

2.5. Characterization of Catalysts

2.5.1. Field Emission Scanning Electron Microscopy (FESEM)

Using FESEM (Zeiss model evo LS15), the morphology of the synthesized catalysts was examined. Energy-dispersive X-ray spectroscopy (EDX) with mapping was conducted to examine the elemental composition or chemical composition of the catalysts. The powder catalysts were utilized in the copper stub along with a two-minute coating of gold film. EDX and FESEM were used to conduct elemental studies of the Mg-modified support with Ni and Ca distribution.

2.5.2. X-ray Diffraction (XRD)

Examining the crystallinity phases using X-ray diffraction (XRD; Bruker D8 Advance) involved exposing the sample to CuK α radiation at a voltage of 40 kV and current of 40 mA while the sample was scanned from 10 to 90 degrees with a step size of 2 min⁻¹.

2.5.3. Thermogravimetric Analysis (TGA)

A thermogravimetric analyzer (Perkin Elmer, Model: STA6000) using N₂ as standard gas was used to conduct thermal analysis of the prepared catalysts in order to calculate the weight loss. At a rate of 30 °C/min, catalysts were heated from room temperature to 800 °C.

2.5.4. CO₂ Sorption Test

The sorption capacity of the catalyst for multiple carbonation–calcination cycles was investigated using the fixed-bed tubular furnace reactor. A catalyst sample weighing 0.1 g was positioned in the reactor's stainless tube at the center and sealed with quartz wool. Before starting the reaction, the catalyst was reduced to 800 °C for 30 min in a 60 mL/min H₂/N₂ (1:1) flow. The outlet gases from the reactor were detected using gas chromatography (GC) equipped with the fixed-bed tubular furnace reactor. The setup for the experiment is shown in Figure 1.

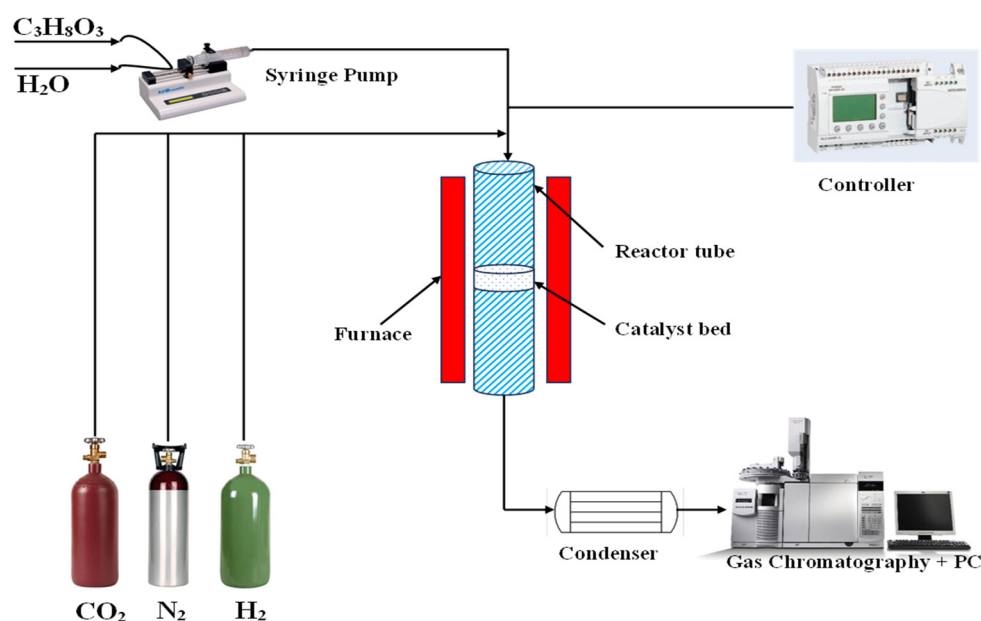


Figure 1. Schematic diagram of the experimental apparatus used to conduct sorption tests [15].

3. Results and Discussion

3.1. Morphology of Catalysts

Figure 2 shows the FESEM surface morphology of calcined 10NMA, 10NCMA-E, and 10NCMA. The FESEM results of fresh 10NMA synthesized using the wet impregnation method are illustrated in Figure 2a,b. Thick plate shapes, with different sizes of irregular and very porous particles in aggregated form, were observed. On the surface of the particles, it was found that Ni metal was dispersed in a specific pattern. In Figure 2c,d, the faces of triangles with a spherical appearance can be identified for the 10NCMA-E catalyst. However, by adding CaO derived from eggshells, the catalyst's porosity was enhanced. Similarly to the 10NMA catalyst, Ni dispersion on the surface of the 10NCMA-E catalyst was observed. However, different size of particles with a wrinkled stone-like shape was observed for the surface morphology of the 10NCMA catalyst as shown in Figure 2e,f. Furthermore, some agglomeration was found in the 10NCMA catalyst. Among all three types of catalysts, 10NCMA-E has the most porous structure compared to the remaining two catalysts, and this is favorable for catalyst activity.

3.2. XRD Analysis

The XRD patterns for the 10NMA, 10NCMA-E, and 10NCMA catalysts are shown in Figure 3. The diffraction patterns at 2θ angles of 25.6, 35.2, 43.9, 52.7, 57.6, 61.2, 66.7, 68.3, and 76.4° are associated with Al₂O₃ [15,52]. The presence of a significant diffraction pattern at 2θ angles of 37.3° and 43.2° refers to the cubic phase of crystalline NiO [15], while at 2θ angles of 36.1 and 64.6°, the peaks refer to the MgAl₂O₄ and NiAl₂O₄, respectively. Therefore, the existence of NiAl₂O₄ in the catalysts increases their resistance to carbon production [15,53]. There was no significant difference among the three types of catalysts found. This was due to the fact that the peaks of CaO could not be identified using XRD for any of the three different types of catalysts. Crystalline phases can only be identified using the XRD technique if they have a composition that is greater than 5% [54].

3.3. Thermogravimetric Analysis

The findings from the TGA investigation on the temperature stability of the catalysts are presented in Figure 4. No significant weight loss was observed for the 10NMA catalyst when it was heated from room temperature to 800 °C. However, weight loss occurred for both the 10NCMA-E and 10NCMA catalysts during the temperature ranges 100–130 °C and 500–520 °C. During the range of 100–130 °C, the weight loss happened due to moisture

content absorbed by the catalysts, while at 500–520 °C the weight loss was due to rapid dehydroxylation and CO₂ release from close-packed carbonate ionic species [55]. At a temperature higher than 520 °C, both catalysts, 10NCMA-E and 10NCMA, became stable and no weight loss was observed.

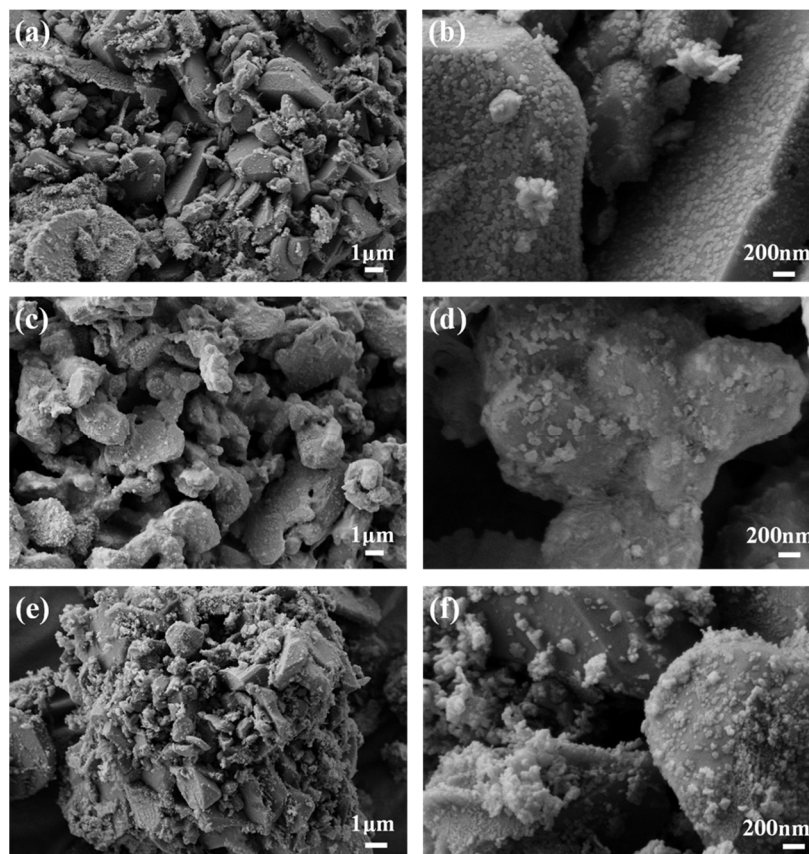


Figure 2. FESEM analysis of calcined catalysts: (a,b) 10NMA, (c,d) 10NCMA-E, and (e,f) 10NCMA.

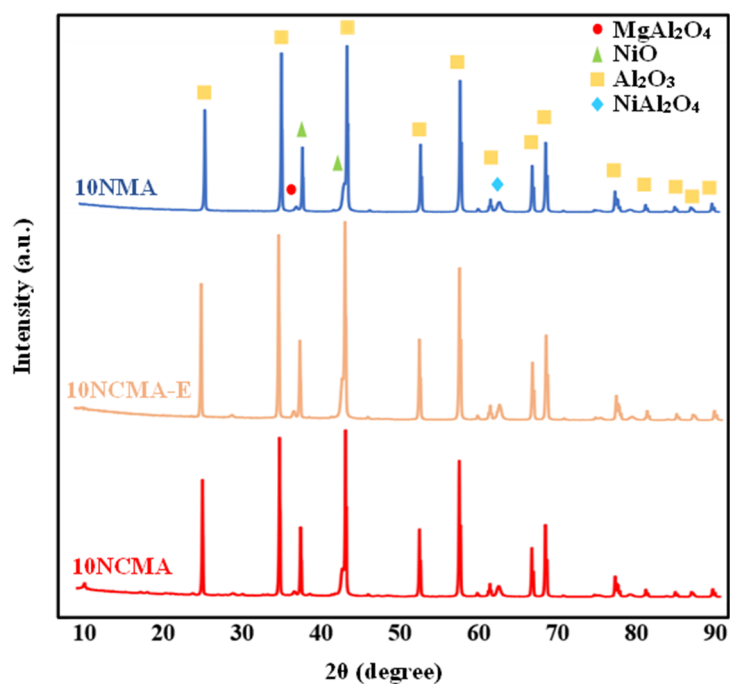


Figure 3. XRD images of 10NMA-, 10NCMA-E-, and 10NCMA-based catalysts.

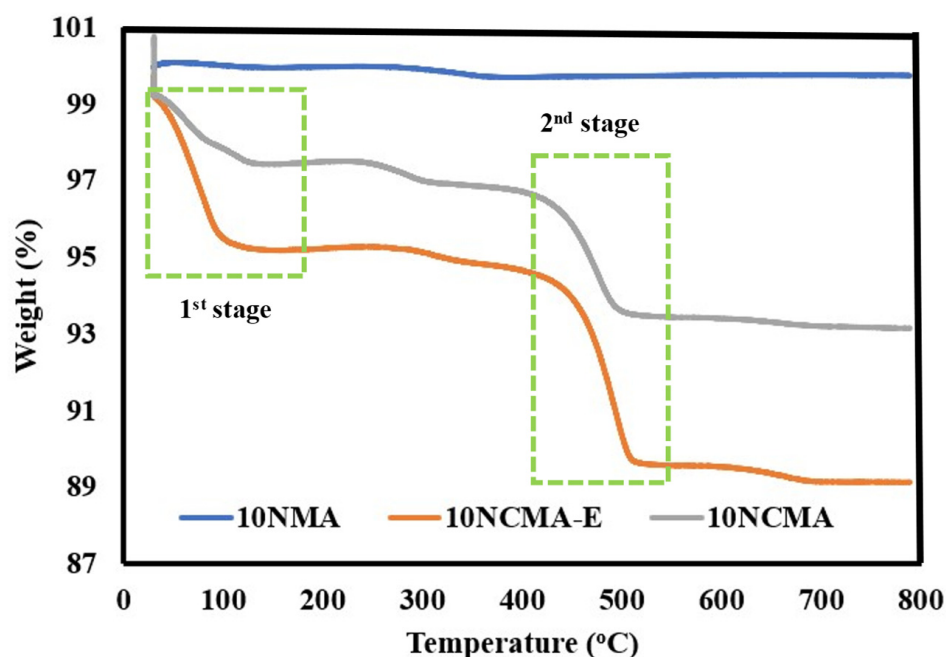


Figure 4. TGA analysis for the 10NMA, 10NCMA-E, and 10NCMA synthesized catalysts.

3.4. CO₂ Sorption Test

Using a fixed-bed tubular reactor, a CO₂ sorption test for the 10NMA, 10NCMA-E, and 10NCMA catalysts was performed and investigated. Gas chromatography was used to investigate the gas composition shortly after the reaction had taken place. During the adsorption process, the reaction temperature was 550 °C, and during the desorption process, the temperature was 800 °C. For the adsorption process, in each of the three different sorption cycles, gas compositions of 30–34% CO₂ and 66–70% N₂ were provided. For the desorption process, however, only N₂ gas was used. Figure 5 presents a comparison of the performance of the 10NMA-, 10NCMA-E-, and 10NCMA-based catalysts during the first adsorption (1A) cycle performed at 550 °C and the first desorption (1D) cycle performed at 800 °C. It was examined that the 10NCMA-based catalyst showed the highest CO₂ sorption ability followed by the 10NCMA-E catalyst during the first carbonation/calcination cycle. When using catalysts based on 10NMA, the amounts of N₂ and CO₂ that were produced at the reactor's outflow during the adsorption process were 67.58% and 32.42%, respectively. These levels of N₂ and CO₂ were quite close to what was delivered in the feed in terms of quantity. This demonstrates that the 10NMA catalyst did not react with the CO₂ gas and that it was unable to adsorb the CO₂ gas. During the desorption process that took place at 800 °C in the presence of pure N₂, GC analysis was able to detect 99.37% N₂ at the exit of the reactor. This indicates there was not a release of CO₂ gas that was anticipated if the catalyst contained CO₂ when it had been previously exposed to CO₂. This confirms that the 10NMA catalyst did not adsorb any CO₂ gas, and, as a result, no release of CO₂ gas occurred when the catalyst was heated at a high temperature. However, in the case of the 10NCMA-E catalyst during the adsorption process, the amounts of N₂ and CO₂ gases noticed at the exit of the reactor were 70.78% and 29.22%, respectively. These concentrations of N₂ and CO₂ were a little smaller in comparison to those that were present at the inlet of the reactor. At the end of the process in which the catalyst was heated at a high temperature in the presence of pure N₂, there was a trace amount (2.23%) of CO₂ gas found at the output of the fixed-bed tubular reactor. This reveals that the CO₂ originated from the catalyst after it was heated to 800 °C, and, as a result, this confirms that the catalyst absorbed CO₂ gas during the adsorption process and then released CO₂ gas during the calcination/desorption process. On the other hand, when a 10NCMA catalyst was simultaneously subjected to N₂ and CO₂ gas, the amount of CO₂ gas that was produced at the output of the reactor was only 3.68%, which was significantly less than the amount that was provided at the input

of the reactor, which was 30%. This suggests the catalyst was successful in adsorbing the CO₂ gas. When the 10NCMA catalyst was heated to a temperature of 800 °C, the amount of adsorbed carbon dioxide that was liberated was 23.88%.

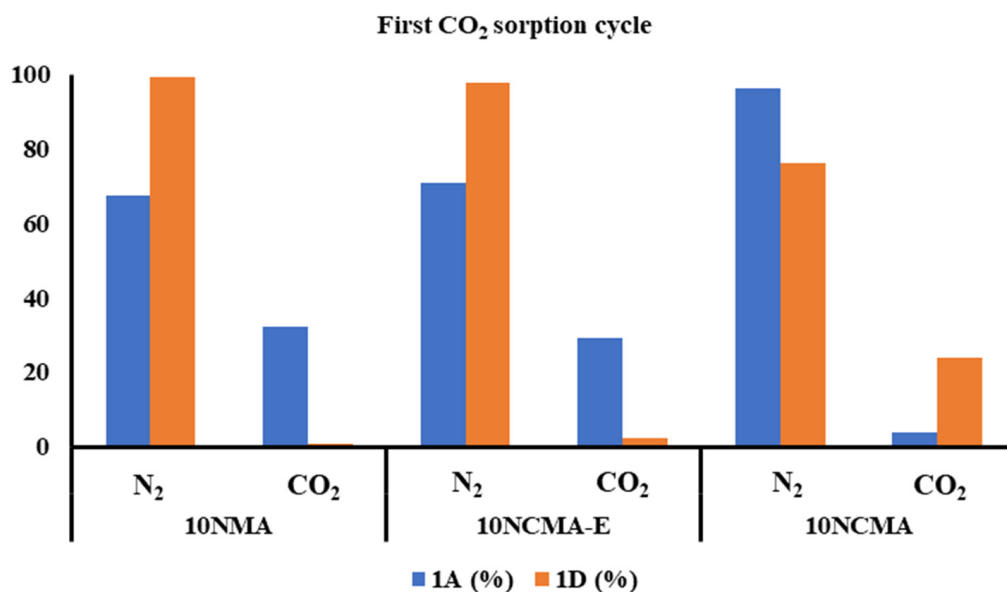


Figure 5. Comparison between 10NMA-, 10NCMA-E-, and 10NCMA-based catalysts during first adsorption (1A) at 550 °C and desorption (1D) at 800 °C cycle.

Figure 6 shows the comparison of the second sorption cycle between the 10NMA, 10NCMA-E, and 10NCMA catalysts. The 10NMA-based catalyst did not show any sorption capacity, comparable to what it showed in the first sorption cycle. Because the gas composition was nearly the same at the input and the outlet of the reactor, it follows that the catalyst did not succeed in capturing any CO₂. In addition, heating the 10NMA catalyst did not cause the release of carbon dioxide, which is evidence that the catalyst is unable to adsorb carbon dioxide. Nevertheless, when a 10NCMA-E-based catalyst was used, the amount of CO₂ that evolved at the reactor's output was lower than the amount that was supplied at the intake. When the catalyst was heated at 800 °C in an atmosphere consisting only of N₂ gas, it caused the catalyst to release CO₂ gas, the composition of which was 90.08% N₂ and 9.92% CO₂. When permitted to interact with a gas that was composed of 66–70% nitrogen and 30–34% carbon dioxide, the catalyst that was generated from commercial CaO (10NCMA) absorbed CO₂ through adsorption. Gas chromatography analysis revealed that there was 97.06% nitrogen gas and 2.94% carbon dioxide gas exiting the reactor. When the 10NCMA catalyst was heated at 800 degrees Celsius in the presence of nitrogen, there was a release of 22.05% CO₂ gas. According to these findings, the 10NCMA-based bifunctional catalyst adsorbed the majority of the CO₂ gas that was present at the temperature of the reaction, but it desorbed the gas during the calcination process.

Figure 7 presents the results of a comparison of the carbonation and calcination activities of the 10NMA-, 10NCMA-E-, and 10NCMA-based catalysts. In the third sorption cycle, it was noted that all three types of catalysts exhibited behavior that was comparable to that which was observed in the first and second sorption cycles. This indicates that the sorption capacity of the 10NCMA-based catalyst was the highest when compared to that of 10NCMA-E and 10NMA. The fact that no CO₂ was adsorbed by the 10NMA catalyst when N₂ and CO₂ were supplied to the system is demonstrated by the desorption process in Figure 7. When the reactor was heated to 800 °C and 100% N₂ gas was introduced, the 10NMA catalyst did not detect any CO₂ gas. However, during the calcination process that followed the carbonation of 10NCMA-E, there was a release of 3.49% CO₂. As a result, the CaO-based catalyst that was generated from wasted chicken eggshells was effective in all three cycles. In the end, the catalyst based on 10NCMA was successful in adsorbing all of

the CO₂ gas that had been supplied. When a 10NCMA-based catalyst was heated at 800 °C for 30 h, 23.37% CO₂ gas was generated.

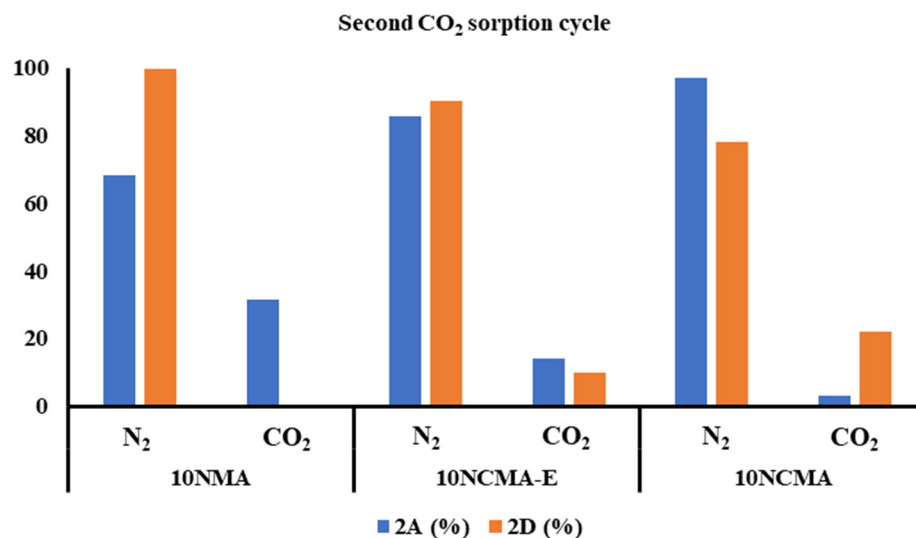


Figure 6. Comparison between 10NMA-, 10NCMA-E-, and 10NCMA-based catalysts during second adsorption (2A) at 550 °C and desorption (2D) at 800 °C cycle.

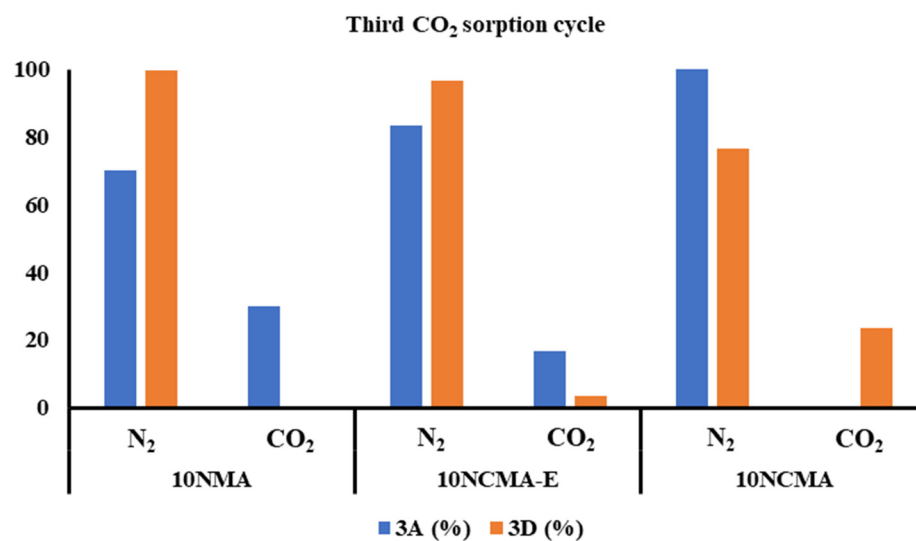


Figure 7. Comparison between 10NMA-, 10NCMA-E-, and 10NCMA-based catalysts during third adsorption (3A) at 550 °C and desorption (3D) at 800 °C cycle.

After analyzing the results from all three cycles, it was determined that the 10NMA catalyst did not exhibit any adsorption ability toward CO₂ gas. This could be attributed to a lack of CaO content in the 10NMA catalyst. Due to the fact that MgO has a low sorption temperature, it is not possible for it to capture CO₂ at temperatures between 500 and 700 °C. This is because MgCO₃ begins to break down around 385 °C, which is lower than the sorption temperature of MgO [56]. The increase in the CaO content of the bifunctional catalyst enhanced its sorption capacity [15,18]. The sorbent releases pure CO₂ through the calcination process (3) in the regeneration cycle, and the sorbent is then available for further CO₂ adsorption during the subsequent reforming cycle [36]. According to the literature, the carbonation and calcination capacity of waste-eggshell-derived calcium oxide nickel-based magnesium- and aluminum-promoted catalysts decreases in consecutive cycles [15]. In the present study, the sorption ability of the 10NCMA-E based catalyst decreased slightly in the third cycle compared to second cycle. However, there is a need to improve the

preparation method for extracting CaO from chicken and duck eggshells. Because the electrical configuration and the structure of catalysts rely on their interaction with the supporting material, the catalytic activity is highly impacted by the support that is used as well as the method that is employed during preparation [15,57].

4. Conclusions

Sorption-enhanced steam reforming is an all-in-one method of producing ultra-pure hydrogen gas via reforming, water gas shift, and carbon dioxide (CO₂) capture. These reactions take place concurrently through a combination of a catalyst and a sorbent for CO₂. This hybrid method offers numerous significant benefits over conventional steam reforming, including improved energy productivity and reduced capital expenditures. The synthesized catalysts showed good physicochemical properties. Among all catalysts, 10NCMA-E showed the highest levels of porosity. Furthermore, it can be seen from the XRD that the 10NCMA-E catalyst has similar characteristics to that prepared using commercial CaO (10NCMA). Among all three types of catalysts, the 10NCMA-based catalyst showed the highest sorption capacity followed by 10NCMA-E during three sorption cycles. The amount of CO₂ released from the 10NCMA-based catalyst during the first, second, and third calcination cycle was 23.88%, 22.05%, and 23.37%, respectively. Following 10NCMA, the amount of CO₂ released from the 10NCMA-E catalyst during the first, second, and third calcination cycle was 2.23%, 9.92%, and 3.49%, respectively. The CO₂ sorption capacity of the NMA-based catalyst was negligible. This is a result of the absence of a CaO sorbent in the NMA-based catalyst. This shows that waste-chicken-and-duck-eggshell-based CaO can also be utilized as a sorbent in catalysts for sorption-enhanced steam reforming. However, the composition of CaO derived from chicken and duck eggshell waste must be purified and optimized. Further studies are required on the stability of the bifunctional catalyst.

Author Contributions: Conceptualization, M.Q. and M.A.; writing—original draft, M.Q.; experimental measurement and formal analysis, K.S.; methodology, M.Q., M.A. and K.S.; supervision, M.A.; writing—review, A.I., S.F., R.S. and M.D. All authors have read and agreed to the published version of the manuscript.

Funding: This research was funded by Yayasan Universiti Teknologi PETRONAS (YUTP, 015LC0-331) and the International Collaborative Research Fund with Kyushu Institute of Technology grant (015ME0-271).

Institutional Review Board Statement: Not applicable.

Informed Consent Statement: Not applicable.

Data Availability Statement: The authors confirm that the data used to support the findings of this study are available within the article.

Acknowledgments: The authors would like to appreciate and acknowledge the Higher Institution Centre of Excellence (HiCoE) grant (015MA0-104) and the Centre for Biofuel and Biochemical Research (CBBR).

Conflicts of Interest: The authors declare no conflict of interest.

References

1. El-Emam, R.S.; Özcan, H. Comprehensive review on the techno-economics of sustainable large-scale clean hydrogen production. *J. Clean. Prod.* **2019**, *220*, 593–609. [[CrossRef](#)]
2. Yan, Y.; Manovic, V.; Anthony, E.J.; Clough, P.T. Techno-economic analysis of low-carbon hydrogen production by sorption enhanced steam methane reforming (SE-SMR) processes. *Energy Convers. Manag.* **2020**, *226*, 113530. [[CrossRef](#)]
3. Shokrollahi Yancheshmeh, M.; Radfarnia, H.R.; Iliuta, M.C. High temperature CO₂ sorbents and their application for hydrogen production by sorption enhanced steam reforming process. *Chem. Eng. J.* **2016**, *283*, 420–444. [[CrossRef](#)]
4. McKinlay, C.J.; Turnock, S.; Hudson, D. *A Comparison of Hydrogen and Ammonia for Future Long Distance Shipping Fuels*; The Royal Institution of Naval Architects: London, UK, 2020.
5. Bossel, U. Does a hydrogen economy make sense? *Proc. IEEE* **2006**, *94*, 1826–1837. [[CrossRef](#)]

6. Requieres, J.; Rabe, S.; Vogel, F.; Truong, T.B.; Filonova, K.; Barrio, V.L.; Cambra, J.F.; Güemez, M.B.; Arias, P.L. Reforming of methane over noble metal catalysts: Catalyst deactivation induced by thiophene. *Catal. Today* **2009**, *143*, 9–16. [[CrossRef](#)]
7. Liu, H.; Liu, S. Life cycle energy consumption and GHG emissions of hydrogen production from underground coal gasification in comparison with surface coal gasification. *Int. J. Hydrogen Energy* **2021**, *46*, 9630–9643. [[CrossRef](#)]
8. Li, X.; Sun, X.; Song, Q.; Yang, Z.; Wang, H.; Duan, Y. A critical review on integrated system design of solar thermochemical water-splitting cycle for hydrogen production. *Int. J. Hydrogen Energy* **2022**, *47*, 33619–33642. [[CrossRef](#)]
9. Qasim, M.; Ayoub, M.; Ghazali, N.A.; Aqsha, A.; Ameen, M. Recent Advances and Development of Various Oxygen Carriers for the Chemical Looping Combustion Process: A Review. *Ind. Eng. Chem. Res.* **2021**, *60*, 8621–8641. [[CrossRef](#)]
10. Qasim, M.; Ayoub, M.; Aqsha, A.; Ghazali, N.A.; Ullah, S.; Ando, Y.; Farrukh, S. Investigation on the Redox Properties of a Novel Cu-Based Pr-Modified Oxygen Carrier for Chemical Looping Combustion. *ACS Omega* **2022**, *7*, 40789–40798. [[CrossRef](#)]
11. Lumbers, B.; Barley, J.; Platte, F. Low-emission hydrogen production via the thermo-catalytic decomposition of methane for the decarbonisation of iron ore mines in Western Australia. *Int. J. Hydrogen Energy* **2022**, *47*, 16347–16361. [[CrossRef](#)]
12. Wang, P.; Zhang, X.; Shi, R.; Zhao, J.; Yuan, Z.; Zhang, T. Light-Driven Hydrogen Production from Steam Methane Reforming via Bimetallic PdNi Catalysts Derived from Layered Double Hydroxide Nanosheets. *Energy Fuels* **2022**, *36*, 11627–11635. [[CrossRef](#)]
13. Lee, T.H.; Jung, U.; Im, H.B.; Kim, K.D.; Kim, J.; Kim, Y.-E.; Song, D.; Koo, K.Y. Comparative evaluation of Ru-coated fccralloloy and SiC monolithic catalysts in catalytic partial oxidation of natural gas for hydrogen production. *J. Ind. Eng. Chem.* **2022**, *110*, 178–187. [[CrossRef](#)]
14. Chaubey, R.; Sahu, S.; James, O.O.; Maity, S. A review on development of industrial processes and emerging techniques for production of hydrogen from renewable and sustainable sources. *Renew. Sustain. Energy Rev.* **2013**, *23*, 443–462. [[CrossRef](#)]
15. Ayesha, M.; Khoja, A.H.; Butt, F.A.; Sikandar, U.; Javed, A.H.; Naqvi, S.R.; ud din, I.; Mehran, M.T. Sorption enhanced steam reforming of methane over waste-derived CaO promoted MgNiAl hydrotalcite catalyst for sustainable H₂ production. *J. Environ. Chem. Eng.* **2022**, *10*, 107651. [[CrossRef](#)]
16. de Castro, T.P.; Silveira, E.B.; Rabelo-Neto, R.C.; Borges, L.E.P.; Noronha, F.B. Study of the performance of Pt/Al₂O₃ and Pt/CeO₂/Al₂O₃ catalysts for steam reforming of toluene, methane and mixtures. *Catal. Today* **2018**, *299*, 251–262. [[CrossRef](#)]
17. Cesário, M.R.; Barros, B.S.; Zimmermann, Y.; Courson, C.; Melo, D.; Kiennemann, A.J.A.C.L. CO₂ sorption enhanced steam reforming of methane using Ni/CaO·Ca₁₂Al₁₄O₃₃ catalysts. *Adv. Chem. Lett.* **2013**, *1*, 292–299. [[CrossRef](#)]
18. Di Giuliano, A.; Girr, J.; Massacesi, R.; Gallucci, K.; Courson, C. Sorption enhanced steam methane reforming by Ni–CaO materials supported on mayenite. *Int. J. Hydrogen Energy* **2017**, *42*, 13661–13680. [[CrossRef](#)]
19. Sikander, U.; Sufian, S.; Salam, M.A. A review of hydrotalcite based catalysts for hydrogen production systems. *Int. J. Hydrogen Energy* **2017**, *42*, 19851–19868. [[CrossRef](#)]
20. Boudjeloud, M.; Boulahouache, A.; Rabia, C.; Salhi, N. La-doped supported Ni catalysts for steam reforming of methane. *Int. J. Hydrogen Energy* **2019**, *44*, 9906–9913. [[CrossRef](#)]
21. Wu, H.; La Parola, V.; Pantaleo, G.; Puleo, F.; Venezia, A.M.; Liotta, L. Ni-based catalysts for low temperature methane steam reforming: Recent results on Ni–Au and comparison with other bi-metallic systems. *Catalysts* **2013**, *3*, 563–583. [[CrossRef](#)]
22. Watanabe, F.; Kaburaki, I.; Shimoda, N.; Satokawa, S. Influence of nitrogen impurity for steam methane reforming over noble metal catalysts. *Fuel Process. Technol.* **2016**, *152*, 15–21. [[CrossRef](#)]
23. Song, H.; Meng, X.; Wang, Z.-J.; Wang, Z.; Chen, H.; Weng, Y.; Ichihara, F.; Oshikiri, M.; Kako, T.; Ye, J. Visible-Light-Mediated Methane Activation for Steam Methane Reforming under Mild Conditions: A Case Study of Rh/TiO₂ Catalysts. *ACS Catal.* **2018**, *8*, 7556–7565. [[CrossRef](#)]
24. Qasim, M.; Ayoub, M.; Aqsha, A.; Zulfiqar, M.J.C.E. Technology, Preparation of Metal Oxide-based Oxygen Carriers Supported with CeO₂ and γ -Al₂O₃ for Chemical Looping Combustion. *Chem. Eng. Technol.* **2021**, *44*, 782–787. [[CrossRef](#)]
25. Qasim, M.; Ayoub, M.; Aqsha, A.; Ghazali, N.A. Investigation and Comparison for the Redox Behavior of Different Metal Oxides (Ni, Fe, Co, Cu, Ce, La, Pr) with and without Gamma-Alumina Support for the Chemical Looping Combustion. *Solid State Technol.* **2020**, *63*, 19450–19460.
26. Ghazali, N.A.; Aqsha, A.; Komiyama, M.; Qasim, M.; Mohd Yusoff, M.H.; Ayoub, M.; Ameen, M.; Tijani, M.M. Comparative Study on Ni/ γ -Al₂O₃ Prepared via Ultrasonic Irradiation and Impregnation Approaches as an Oxygen Carrier in Chemical Looping Combustion. *Ind. Eng. Chem. Res.* **2021**, *60*, 13542–13552. [[CrossRef](#)]
27. He, M.; Zhang, J.; Shi, Z.; Liu, F.; Li, X. Synthesis of hydrotalcite-like compounds from blast furnace slag: The effect of synthesis parameters on structure and crystallinity. In *Energy Technology 2015: Carbon Dioxide Management and Other Technologies*; Springer: Berlin/Heidelberg, Germany, 2015; pp. 325–331.
28. Trimm, D.L. Catalysts for the control of coking during steam reforming. *Catal. Today* **1999**, *49*, 3–10. [[CrossRef](#)]
29. Alshafei, F.H.; Minardi, L.T.; Rosales, D.; Chen, G.; Simonetti, D.A. Improved Sorption-Enhanced Steam Methane Reforming via Calcium Oxide-Based Sorbents with Targeted Morphology. *Energy Technol.* **2019**, *7*, 1800807. [[CrossRef](#)]
30. Kwon, Y.M.; Chae, H.J.; Cho, M.S.; Park, Y.K.; Seo, H.M.; Lee, S.C.; Kim, J.C. Effect of a Li₂SiO₃ phase in lithium silicate-based sorbents for CO₂ capture at high temperatures. *Sep. Purif. Technol.* **2019**, *214*, 104–110. [[CrossRef](#)]
31. Lee, S.C.; Kim, M.J.; Kwon, Y.M.; Chae, H.J.; Cho, M.S.; Park, Y.K.; Seo, H.M.; Kim, J.C. Novel regenerable solid sorbents based on lithium orthosilicate for carbon dioxide capture at high temperatures. *Sep. Purif. Technol.* **2019**, *214*, 120–127. [[CrossRef](#)]
32. Ruhaimi, A.H.; Aziz, M.A.A.; Jalil, A.A. Magnesium oxide-based adsorbents for carbon dioxide capture: Current progress and future opportunities. *J. CO₂ Util.* **2021**, *43*, 101357. [[CrossRef](#)]

33. Mendoza-Nieto, J.A.; Tehuacanero-Cuapa, S.; Arenas-Alatorre, J.; Pfeiffer, H. Nickel-doped sodium zirconate catalysts for carbon dioxide storage and hydrogen production through dry methane reforming process. *Appl. Catal. B Environ.* **2018**, *224*, 80–87. [CrossRef]
34. Martavaltzi, C.S.; Pefkos, T.D.; Lemonidou, A.A. Operational Window of Sorption Enhanced Steam Reforming of Methane over CaO–Ca₁₂Al₁₄O₃₃. *Ind. Eng. Chem. Res.* **2011**, *50*, 539–545. [CrossRef]
35. Nawar, A.; Ali, M.; Khoja, A.H.; Waqas, A.; Anwar, M.; Mahmood, M. Enhanced CO₂ capture using organic acid structure modified waste eggshell derived CaO sorbent. *J. Environ. Chem. Eng.* **2021**, *9*, 104871. [CrossRef]
36. Broda, M.; Manovic, V.; Imtiaz, Q.; Kierzkowska, A.M.; Anthony, E.J.; Müller, C.R. High-Purity Hydrogen via the Sorption-Enhanced Steam Methane Reforming Reaction over a Synthetic CaO-Based Sorbent and a Ni Catalyst. *Environ. Sci. Technol.* **2013**, *47*, 6007–6014. [CrossRef]
37. Aloisi, I.; Jand, N.; Stendardo, S.; Foscolo, P.U. Hydrogen by sorption enhanced methane reforming: A grain model to study the behavior of bi-functional sorbent-catalyst particles. *Chem. Eng. Sci.* **2016**, *149*, 22–34. [CrossRef]
38. Wang, C.; Sun, N.; Zhao, N.; Wei, W.; Sun, Y.; Sun, C.; Liu, H.; Snape, C.E. Coking and deactivation of a mesoporous Ni–CaO–ZrO₂ catalyst in dry reforming of methane: A study under different feeding compositions. *Fuel* **2015**, *143*, 527–535. [CrossRef]
39. Chalermwat, N.; Rattanaprapanporn, R.; Chalermnsinuan, B.; Poompradub, S.J. Natural Calcium-Based Residues for Carbon Dioxide Capture in a Bubbling Fluidized-Bed Reactor. *Chem. Eng. Technol.* **2018**, *41*, 428–435. [CrossRef]
40. Wang, J.; Yang, Y.; Jia, Q.; Shi, Y.; Guan, Q.; Yang, N.; Ning, P.; Wang, Q.J.C. Solid-waste-derived carbon dioxide-capturing materials. *ChemSusChem* **2019**, *12*, 2055–2082. [CrossRef]
41. Kannan, M.B.; Ronan, K. Conversion of biowastes to biomaterial: An innovative waste management approach. *Waste Manag.* **2017**, *67*, 67–72. [CrossRef]
42. Salaudeen, S.A.; Acharya, B.; Dutta, A. CaO-based CO₂ sorbents: A review on screening, enhancement, cyclic stability, regeneration and kinetics modelling. *J. CO₂ Util.* **2018**, *23*, 179–199. [CrossRef]
43. Waheed, M.; Yousaf, M.; Shehzad, A.; Inam-Ur-Raheem, M.; Khan, M.K.I.; Khan, M.R.; Ahmad, N.; Abdullah; Aadil, R.M. Channelling eggshell waste to valuable and utilizable products: A comprehensive review. *Trends Food Sci. Technol.* **2020**, *106*, 78–90. [CrossRef]
44. Canadian Food Innovators. Turning Egg Shells into a Functional Food Ingredient. Canadian Food Innovators. 2015. Available online: <https://canadianfoodinnovators.ca/project/turning-egg-shells-into-a-functional-food-ingredient> (accessed on 19 August 2023).
45. Salaudeen, S.A.; Tasnim, S.H.; Heidari, M.; Acharya, B.; Dutta, A. Eggshell as a potential CO₂ sorbent in the calcium looping gasification of biomass. *Waste Manag.* **2018**, *80*, 274–284. [CrossRef] [PubMed]
46. Habte, L.; Shiferaw, N.; Mulatu, D.; Thenepalli, T.; Chilakala, R.; Ahn, J.W.J.S. Synthesis of nano-calcium oxide from waste eggshell by sol-gel method. *Sustainability* **2019**, *11*, 3196. [CrossRef]
47. Ahmad, R.; Rohim, R.; Ibrahim, N.J. Properties of waste eggshell as calcium oxide catalyst. *Appl. Mech. Mater.* **2015**, *754*, 171–175. [CrossRef]
48. Daengprok, W.; Garnjanagoonchorn, W.; Mine, Y. Fermented pork sausage fortified with commercial or hen eggshell calcium lactate. *Meat Sci.* **2002**, *62*, 199–204. [CrossRef]
49. Nakano, T.; Ikawa, N.I.; Ozimek, L. Chemical composition of chicken eggshell and shell membranes. *Poult. Sci.* **2003**, *82*, 510–514. [CrossRef]
50. Mittal, A.; Teotia, M.; Soni, R.K.; Mittal, J. Applications of egg shell and egg shell membrane as adsorbents: A review. *J. Mol. Liq.* **2016**, *223*, 376–387. [CrossRef]
51. Baláz, M. Eggshell membrane biomaterial as a platform for applications in materials science. *Acta Biomater.* **2014**, *10*, 3827–3843. [CrossRef]
52. Mohammed, A.A.; Khodair, Z.T.; Khadom, A.A. Preparation and investigation of the structural properties of α -Al₂O₃ nanoparticles using the sol-gel method. *Chem. Data Collect.* **2020**, *29*, 100531. [CrossRef]
53. Rahbar Shamskar, F.; Rezaei, M.; Meshkani, F. The influence of Ni loading on the activity and coke formation of ultrasound-assisted co-precipitated Ni–Al₂O₃ nanocatalyst in dry reforming of methane. *Int. J. Hydrogen Energy* **2017**, *42*, 4155–4164. [CrossRef]
54. Gayán, P.; Forero, C.R.; Abad, A.; de Diego, L.F.; García-Labiano, F.; Adánez, J. Effect of Support on the Behavior of Cu-Based Oxygen Carriers during Long-Term CLC Operation at Temperatures above 1073 K. *Energy Fuels* **2011**, *25*, 1316–1326. [CrossRef]
55. Kong, X.; Zheng, R.; Zhu, Y.; Ding, G.; Zhu, Y.; Li, Y.-W. Rational design of Ni-based catalysts derived from hydrotalcite for selective hydrogenation of 5-hydroxymethylfurfural. *Green Chem.* **2015**, *17*, 2504–2514. [CrossRef]
56. Yan, C.-F.; Hu, E.-Y.; Cai, C.-L. Hydrogen production from bio-oil aqueous fraction with in situ carbon dioxide capture. *Int. J. Hydrogen Energy* **2010**, *35*, 2612–2616. [CrossRef]
57. Azancot, L.; Bobadilla, L.F.; Santos, J.L.; Córdoba, J.M.; Centeno, M.A.; Odriozola, J.A. Influence of the preparation method in the metal-support interaction and reducibility of Ni-Mg-Al based catalysts for methane steam reforming. *Int. J. Hydrogen Energy* **2019**, *44*, 19827–19840. [CrossRef]

Disclaimer/Publisher’s Note: The statements, opinions and data contained in all publications are solely those of the individual author(s) and contributor(s) and not of MDPI and/or the editor(s). MDPI and/or the editor(s) disclaim responsibility for any injury to people or property resulting from any ideas, methods, instructions or products referred to in the content.